Efficient Modeling and Estimation of Group Music and Dance Happiness via Intelligent Wearable Devices

Qian Wang[1] 🆔

Abstract

Smart wearable items are becoming more well recognized and are steadily making their way into people's lives as a result of the ongoing advancement of technology and people's growing concern for their health. In this work, we investigate the stimulation of physiological signals and the level of happiness indicated by people's emotions using the linkage of smart gadgets and biological data. To reduce motion artifacts from wearable PPGs, we first suggest a sparse representation-based approach. To address the issue of poor model generalization brought on by individual signal differences (inter- and intra-individual) in human ECG data, a wearable ECG individual signal difference reduction technique based on Balanced Distribution Domain Adaptive (BDA) is also suggested. In addition to making a significant contribution to the advancement of intelligent control technology, medicine, and other fields, it provides an effective baseline for research on the satisfaction level of group music and dancing based on physiological signals.

Keywords Intelligence · Wearable devices · Music and dance · Sports

1 Introduction

Dance and music may be employed as a kind of exercise that lasts a lifetime. In addition to enhancing emotional and physical health, music and dance also have the power to regulate daily life, foster better interpersonal relationships, and fill individuals with vigor and vitality. According to psychologists, the emotional responses of the elderly can be broadly categorized as melancholy, sadness, anxiety, loneliness, guilt, helplessness, and anger, and the cognitive changes can be broadly categorized as pessimism, short attention span, hopelessness, helplessness, uselessness, low value, and, in some cases, delusions, fantasies, or suicidal thoughts, which are more common in the elderly than in other age groups [1]. Compared to other age groups, the elderly are more prone to have these symptoms [2]. According to the survey, it is well known that senior people frequently experience temporary anxiety symptoms. If psychological issues are effectively handled, elderly people's bad behaviors and social issues can be alleviated [3]. Female seniors who actively engage in social activities have been shown to live longer, and group music and dance activities give seniors a new platform to express their social roles while also giving them a place to confide in and communicate with one another, effectively reducing loneliness and raising happiness levels. However, it is very important to accurately capture the real physiological excitement of people to music and dance, as well as the pleasurable biological stimulation.

Physiological signal analysis and processing algorithms for wearable technology have advanced quickly in recent years, making significant contributions to domains of human health monitoring such heart rate estimates of human activity and emotion identification [4, 5]. In the human health monitoring system, as seen in Fig. 1, wearable devices like smart watches and bracelets are used to gather physiological signals from the body, such as photoplethysmography (PPG) and electrocardiogram (ECG), before transmitting the information to a distant server. Finally, the analysis and processing of physiological information allows for the perception of the human body's state of health [6]. The human health monitoring system can help reduce the scarcity of medical resources brought on by China's massive population base and growing aging rate in addition to offering low-load and long-term continuous daily health monitoring for the monitored [7]. Consequently, developing algorithms for

✉ Qian Wang
  107622012010044@xjnu.edu.cn

1   School of Music, Xinjiang Normal University,
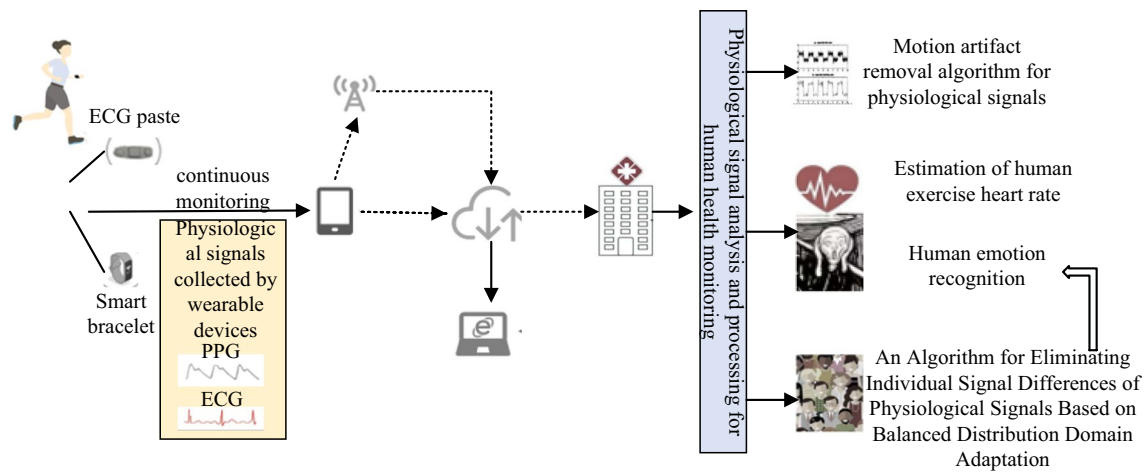   Urumqi 830054, China

Fig. 1 Human health monitoring system based on physiological signal analysis and processing

physiological data analysis and processing for wearable technology has significant scientific and societal implications.

A human health monitoring system can not only provide low-load, long-term continuous daily health monitoring for the monitored individuals, but also alleviate the shortage of medical resources due to the huge population base and the deepening aging in China. This paper proposes a wearable ECG individual signal discrepancy elimination algorithm based on BDA. The effectiveness of this algorithm in eliminating individual signal differences in ECG is verified in an emotion recognition experiment based on an open dataset. Our model can provide effective help for accurate estimation of emotions and group activities, not only limited to music and dance. Therefore, it is of great scientific and social importance to conduct research on physiological signal analysis and processing algorithms for wearable devices.

2 Related Work

One of the sports that older people engage in is aerobic exercise of low-to-moderate intensity, and one of them is music and dance, which forms a regular acoustic vibration through changes in tone and melody, which is a benign stimulus for the human body and has a direct effect on the brain, and this physical energy can cause the tissue cells to resonate harmoniously, resulting in physiological and psychological responses [8, 9]. Al-Turjman et al. [10] indicate that older adults who engage in regular exercise have significantly higher subjective health status (self-perceived health, recuperation, mental health, and stress management) than those who do not exercise. He et al. [11] interviewed older adults who participated in square dancing and concluded that they had higher happiness scores and all had good interpersonal relationships and fulfilling social lives. Kaur et al. [12]

noted that female older adults who exercised consistently had fewer functional limitations in health, better daily functioning, better exercise related self-efficacy, and fewer falls. Shen et al. [13] indicated that as older adults participated in group leisure activities more frequently, their physical and mental health and vitality tended to increase. By analyzing the current status of domestic and international research, this section attempts to show the trend of related research areas.

2.1 Product Design of Physiological Data

The word "emotion" is derived from the Greek word "pathos" and was first used to express people's feelings about tragedy [14]. Emotion plays a central role in a range of intelligent activities, such as perception, decision-making, logical reasoning, and social interaction, and some studies even show that "80%" of human communication is emotional information [15]. Because of the significance of emotion in human communication, affective computing is an essential part of the human–computer interaction process and an important breakthrough in making machines intelligent [16, 17]. Emotional computing and understanding aims to give computer systems the ability to recognize, understand, express, and adapt to human emotions to build a harmonious human–computer environment, and to make computers more intelligent and comprehensive [18, 19]. Depending on the input signal, affective computing and understanding encompasses different research directions. In addition, unlike the short-term and sparse characteristics of visual or speech emotion signals, physiological signals are long-time continuous signals that can work continuously in the absence or failure of traditional visual and speech signals, and thus can effectively enhance human–computer interaction or interpersonal interaction.

2.2 Methods Related to Emotion Measurement

According to the current mainstream research, models for measuring emotions are mainly divided into basic emotion theories (categorical models) and dimensional emotion theories. The basic emotion theory is a collection of basic and universal fundamental emotions [20, 21]. In recent years, physiological data mainly include peripheral physiological measurements (e.g., heart rate, respiration, electromyography, dermatography, skin temperature, etc.) and central nervous system measurements (e.g., EEG and functional magnetic resonance imaging) [22, 23]. Southwestern University in China has also done a lot of work on emotion recognition based on human physiological data, and considers physiological data as a very useful feature for identifying human emotions [24]. Measuring physiological signals is the first step in building a system that can automatically identify physiological patterns related to emotions. In a broad sense, all bodily changes can be considered as changes in physiological signals, including brain activity, facial expressions, voice patterns, and body chemistry. In this paper, we focus on continuous physiological signals measured from the skin surface, which can reflect the activity of the autonomic nervous system. Next, we will discuss the characteristics of cardiac activity (heart rate and heart rate variability), blood pressure, skin conductivity, surface electromyography, respiration, pulse, and other physiological signals.

With the rapid development of network technology and intelligent hardware, wearable devices have become a hot spot for current research. The application of wearable devices in the field of human health monitoring provides a new path for disease monitoring and diagnosis, and has become a hot spot in the current medical device innovation. Based on this, this paper briefly introduces the current application status and development trend of wearable devices in the field of music and dance well-being of elderly people.

3 Methodology

3.1 PPG Motion Artifact Removal Based on Sparse Representation

The purpose of this section is to remove motion artifacts (MA) of PPG using sparse representation (SR) based on the selected dictionary. It should be noted that this paper sets the dictionary form according to the strength of MA in the original signal to effectively express the original signal. In this part, we first introduce the binary decision based on correlation (used to determine whether the original PPG signal contains strong MA), and then describe the PPG MA removal algorithm based on sparse representation. The purpose of correlation-based decision-making is to determine

whether the original PPG signal contains strong MA by calculating the correlation coefficient between the STFT amplitude of the original PPG signal and the STFT amplitude of the acceleration signal. If the calculated Pearson correlation coefficient is not high, then the original PPG signal does not contain strong MA (that is, the PPG signal is considered clean). In this case, to avoid interference of MA dictionary atoms (from acceleration signal), MA dictionary R is not used. First, the STFT amplitude of PPG signal and acceleration signal is calculated. Specifically, this paper uses STFT to convert the original PPG signal s_{raw} and acceleration signal a_{raw} into STFT amplitude domain, as shown in Eqs. (1) and (2)

$$\mathbf{X} = \left| \mathrm{STFT}(\mathbf{s}_{raw}) \right| \tag{1}$$

$$\mathbf{A} = \left| \mathrm{STFT}(\mathbf{a}_{raw}) \right| \tag{2}$$

where $X \in R\ m \times N$ is the STFT amplitude of s_{raw}, and $A \in R\ m \times N$ is the STFT amplitude of a_{raw}. M represents the component in the frequency range of 0–5 Hz (the frequency range of heart rate) in the STFT domain. N represents the number of time windows. The acceleration signal a_{raw} is the addition of three-axis acceleration signals after band-pass filtering. Second, the matrix X is converted into a column vector $x \in R(m * n) \times 1$, that is, x is composed of column vectors in matrix X. Similarly, matrix A is transformed into a column vector $a \in R(m * n) \times 1$, that is, a is composed of column vectors in matrix A. M · n represents the multiplied value of m and n. Finally, measure the Pearson correlation coefficient between x and a whether the pcorr meets the following conditions, as shown in Eq. (3):

$$\left| \rho_{corr} \right| \leq \Delta_{corr}. \tag{3}$$

Including Δ Corr is a preset threshold. If ρcorr meets Eq. (3), the original PPG signal is determined to be clean (or contains weak MA). At this time, only the PPG dictionary is used, and the MA dictionary is not used, which is expressed as Eq. (4)

$$D = \tilde{R} \tag{4}$$

If Pcorr cannot meet the Eq. (3), and the original PPG signal is determined to be unclean (or contains strong MA). At this time, both PPG dictionary and MA dictionary will be used, expressed as Eq. (5):

$$D = [\tilde{R}R]. \tag{5}$$

where D represents the dictionary used in the MA removal algorithm of sparse representation. (2) The sparse representation PPG motion artifact removal sparse representation PPG motion artifact (MA) removal algorithm aims to

remove MA from the original PPG signal using the sparse representation algorithm. Sparse representation is a new signal processing technology, which has shown great potential in many applications. The sparse representation algorithm can be used for PPG and acceleration signals, because PPG signal and acceleration signal (MA reference signal) are sparse in a specific domain; the regularity of PPG and acceleration signals indicates that these two signals can be well represented. If an original PPG signal contains strong MA, this paper assumes that the STFT amplitude of the original PPG signal $x \in R(m * n) \times 1$, STFT amplitude $s \in R$ (m · n) of clean PPG signal $\times 1$, and STFT amplitude of MA $m \in R(m * n) \times 1$ and 1. This assumption can be expressed as Eq. (6)

$$X = s + m. \tag{6}$$

This assumption is like the assumption of speech enhancement. It is the sum of the spectrum amplitude of the original noisy speech signal that can be approximately regarded as speech signal and noise signal. Based on this assumption, if the original PPG signal contains strong MA, then $D = [R \ \tilde{R}]$, That is, the dictionary D used in sparse representation is determined by the PPG dictionary $\tilde{R}$ and MA dictionary R. At this time, the optimization problem in Eq. (7) can be used to remove MA. The purpose of sparse representation is to use a linear combination of a small number of dictionary atoms (atoms selected from dictionary D that are related to the original PPG signal x), the sparse coefficient is obtained by approximating the original PPG signal x with a lower error. The amplitude of clean PPG is estimated by the sparse coefficient obtained, and the contribution of MA is ignored, so MA is removed, and the denoised PPG signal is obtained. According to the form of D, the sparse representation algorithm includes two cases. On the one hand, if $D = \tilde{R}$, the purpose of sparse representation algorithm is to use the dictionary $\tilde{R}$ from the clean PPG linear combination of dictionary atoms. In this case, to remove MA, the obtained MA dictionary atom is ignored. Only the sparse coefficient corresponding to the clean PPG signal is used to estimate the clean PPG amplitude, and the clean PPG signal is reconstructed combining the phase of the original PPG signal to obtain the denoised PPG signal. The optimization problem of sparse representation algorithm is expressed as

$$\min_{\mathbf{c}} \|\mathbf{x} - \mathbf{D}\|_2$$
$$\text{s.t.} \|\mathbf{c}\|_0 \leq K, \tag{7}$$

where x represents the STFT amplitude of the original PPG signal after band-pass filtering. D is the dictionary after the decision using correlation $(D = \tilde{R}$ or $D = [R \ \tilde{R}])$ ° K is a small positive integer. C is a sparse coefficient vector. $c = c \ \tilde{R}$ or $c = [\tilde{C} \ r \ cr]$ T, where $\tilde{C}$ R and cr correspond to PPG dictionary $\tilde{R}$ And MA dictionary R. This optimization problem aims to obtain a sparse coefficient vector c, so that when the coefficient vector is sparse, the linear combination of a few dictionary atoms (the product of dictionary atoms and sparse coefficients) in dictionary D can approximately represent the original PPG signal x. The above optimization problem, Eq. (7), can be solved by using many algorithms, such as orthogonal matching pursuit OMP and base pursuit noise reduction. These algorithms use different criteria and steps to solve problems. Because OMP algorithm has low computational complexity and is simple to implement, this paper chooses OMP algorithm in the experiment. OMP is an iterative algorithm for selecting atoms from dictionaries. After the OMP algorithm is used to solve the optimization problem represented by Eq. (7), a sparse coefficient vector c is obtained in this paper. Then, the estimated STFT amplitude is corresponding to the denoised (clean) PPG signal $\hat{S}$. It can be obtained in the following way, as shown in Eq. (8):

$$\hat{S} = \hat{R}c_{\tilde{r}}^T. \tag{8}$$

Among them, $\hat{S}$ S can be converted into a denoised PPG signal in the time domain. Vector $\hat{S} \in R$ (m·n) $\times 1$ is converted to matrix $\hat{S} \in R$ m $\times$ n, where the matrix under the STFT field $\hat{S}$ It can be converted into a denoised PPG signal in the time domain [by the following Eq. (9)]. Finally, based on the PPG signal $\hat{S}$ in the STFT amplitude domain and the phase of the original PPG signal, $\hat{S}$ is converted into the denoised PPG signal (signal in the time domain) srecon through the inverse STFT transform. The denoised PPG signal srecon will be used in the following heart rate peak tracking algorithm. The process of inverse STFT transformation can be expressed, as shown in Eq. (9). Where ISTFT represents the inverse STFT transform

$$S_{RECON} = ISTFT(\hat{S}). \tag{9}$$

3.2 Wearable ECG Difference Elimination Algorithm

In this section, a balanced BDA-based wearable ECG individual signal disparity elimination algorithm is proposed for sentiment recognition scenarios, which improves the performance of online sentiment recognition by overcoming inter-individual signal disparity as well as intra-individual signal disparity simultaneously. The algorithm uses the BDA algorithm [25] to reduce inter-individual signal differences, obtains a shared subspace of source and target user data, and trains an emotion classifier (based on source user data) for the target user in the shared subspace. At the same time, the Online Data Adaptation (ODA) algorithm is used to reduce the intra-individual signal differences, so that the time-varying ECG signals arriving online can be adapted to improve the online recognition performance. Figure 2 shows the framework of a wearable ECG individual signal
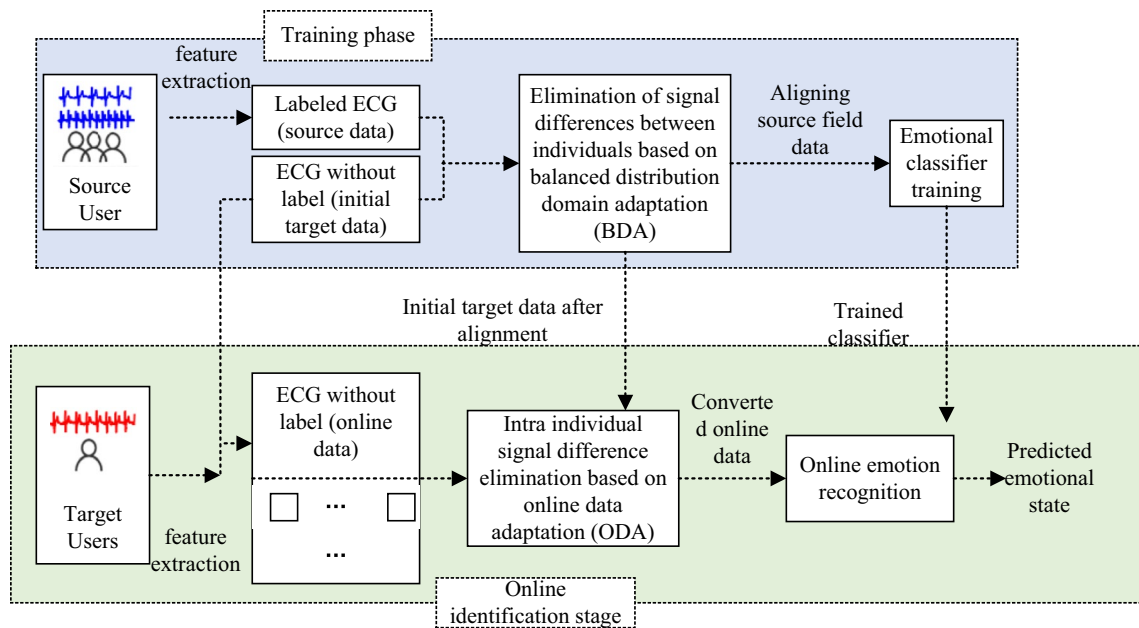
Fig. 2 Wearable ECG individual signal difference elimination algorithm framework for emotion recognition

difference elimination algorithm for emotion recognition. It mainly includes four parts: signal difference elimination between individuals based on balanced BDA, emotion classifier training, intra-individual signal difference elimination based on ODA, and online emotion recognition.

The BDA algorithm is used to learn a shared subspace and prepare for the training part of the emotion classifier. Figure 3 shows the principle of BDA-based inter-individual signal difference elimination algorithm. It can be seen from the figure that BDA makes the data of the two fields distributed and aligned in the shared subspace. BDA is a UDA algorithm, which can not only minimize the difference between edge distribution and conditional distribution, but also adaptively adjust the importance of each distribution. The BDA algorithm aims to minimize the difference between the source domain ECG data and the target domain ECG data, as shown in Eq. (10)

$$\frac{\min}{P_r}\mathrm{tr}\left(\mathbf{P}_r\mathbf{X}\left((1-\theta)\mathbf{M}_0+\theta\sum_{c=1}^{C}\mathbf{M}_c\right)\mathbf{X}^T\mathbf{P}_r\right)+\lambda\|\mathbf{P}_r\|_F^2 \quad (10)$$
$$s.t.\mathbf{P}_r^T\mathbf{X}\mathbf{H}\mathbf{X}^T\mathbf{P}_r=\mathbf{I}, 0\le\theta\le 1.$$

Because of the nonstationary of ECG, the ECG changes with time, resulting in differences between the online ECG data and the initial data of the same target user (intra-individual signal differences), resulting in the classifier f obtained in the previous part may not be applicable to the newly arrived online data. As shown in Fig. 3, although

Pr obtained by BDA can map online data to a shared subspace (i.e., Fig. 3c). The purpose of ODA algorithm is to adaptively adapt time-varying ECG signals by reducing the signal difference within individuals (the difference between the online data of the same target user and the initial target data), to improve the performance of online emotion recognition. Specifically, the algorithm reduces the difference of second-order statistical characteristics between online data and initial target data, the time-varying ECG signals arriving online are adaptive to improve the online learning ability of the recognition model.

4 Experiments

4.1 Datasets

In the experiment, a variety of typical pseudo-periodic motion data sets are used. The six typical pseudo-periodic movements are walking, fast running, waving, arm swinging, elliptical machine, and squatting. These movements are related to hand movements, which are the main source of MA. Figure 4 shows the schematic diagram of six common fitness exercises: walking, fast running, waving, arm swinging, elliptical machine, and squatting. Figure 5 shows the hardware settings for collecting data. Figure 5a shows the hardware frame diagram during data acquisition, and Fig. 5b shows a subject with hardware. Among them, ECG sensor is used to obtain three lead ECG: LA, RA, and LL (LA and RA are placed in the left and right chest, and

Fig. 3 Schematic diagram of signal difference elimination algorithm between individuals based on BDA and intra-individual signal difference elimination algorithm based on ODA
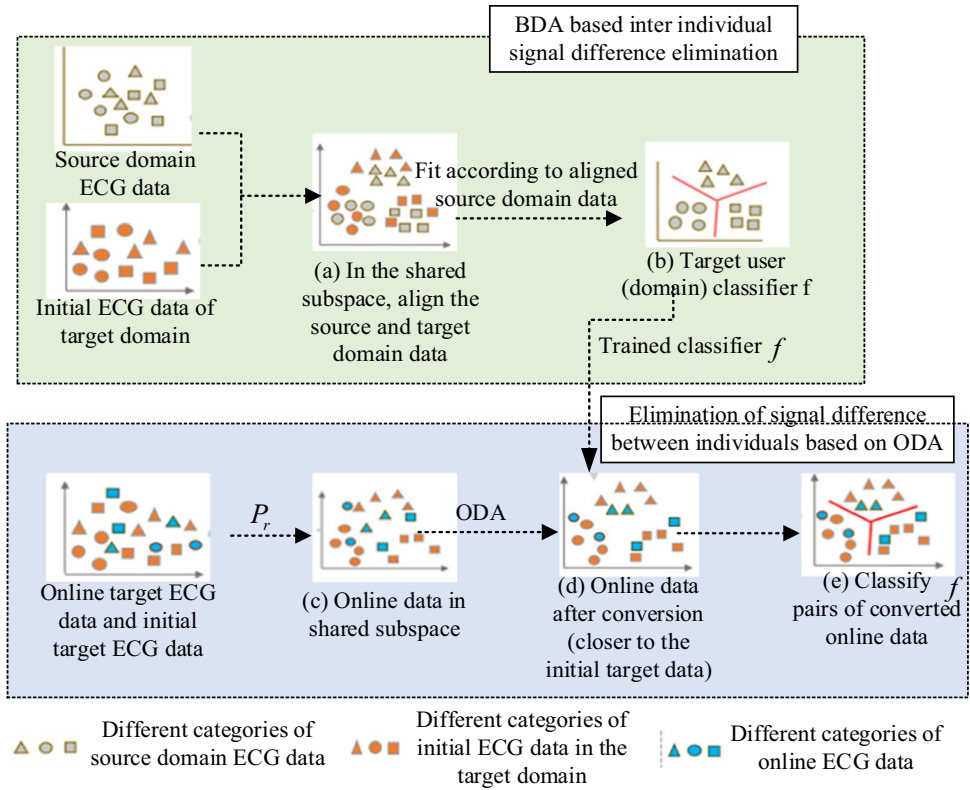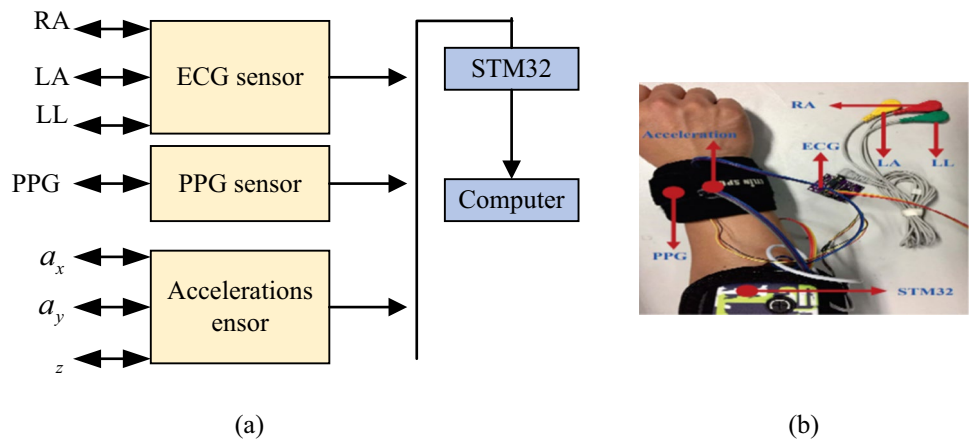

Fig. 4 Schematic diagram of six typical pseudo-periodic motions. **a** Walking; **b** run fast; **c** wave; **d** swing arm; **e** elliptical training; **f** squat

Fig. 5 Hardware settings for data acquisition. **a** Block diagram of hardware settings for data acquisition. **b** A subject wearing hardware

LL lead is placed in the left lower abdomen); the reflective pulse oximeter sensor with green LED is used to collect PPG signals; the ADXL345 sensor is used to collect the three-axis acceleration signal. Finally, all data of the above sensors are processed through STM32 and transmitted to the host for data analysis and processing.

The six datasets used in this chapter were collected, while subjects performed six typical pseudo-periodic exercises.

Specifically, the Running dataset contains Walking and Running Fast; Beckoning contains Reckoning; Swing Arm contains Swing Arm; Elliptical Trainer contains Elliptical Machine; Deep Keen Bend contains Squat; and Mixture contains Reckoner, Swing Arm, and Squat.

The Running dataset was first presented in the literature [26]. It was collected from 12 subjects (aged 18–35 years) and 12 records were obtained. For each individual, three signals were acquired simultaneously, namely, a single-pass photoelectric volumetric pulse-wave signal (PPG), a triaxial acceleration signal, and an ECG. These signals were sampled at a frequency of 125 Hz and were acquired for approximately five minutes for each subject. Specifically, subjects first walked at 12 km/h for 0.5 min, then ran at 68 km/h for 1 min, then ran at 1215 km/h for 1 min, and finally walked at 12 km/h for 0.5 min.

The other five datasets (Beckoning, Swing Arm, Elliptical Trainer, Deep Keen Bend, and Mixture) involved exercises, such as handstands, arm swings, elliptical training, and squats. The first four datasets were collected from 9 subjects (aged 18–35 years), resulting in 9 records. The Mixture dataset was collected from 4 subjects, resulting in four records. Each record lasted approximately 4 min. For each subject, the signals collected simultaneously included a single-channel PPG signal, a triaxial acceleration signal, and an ECG signal.

The other five datasets are described in detail below.

The Beckoning dataset contains the beckoning action. During the acquisition, subjects rested for 0.5 min at the beginning and end of the acquisition. At other times, subjects performed the hand wave for 3 min. The hand-waving motion was very similar to the common mascot, the maneki-neko (depicting a cat waving with an upright paw).

The Swing Arm dataset contains arm-swinging movements. During the acquisition, subjects rested for 0.5 min at the beginning and end of the acquisition. At other times, the subject swings the arm with the sensor back and forth for 3 min at an angle of approximately 60°.

The Elliptical Trainer data set was collected from subjects during elliptical training. At the time of acquisition, subjects first rested for 0.5 min, then exercised on the elliptical machine for 1 min at 46 km/h, followed by 1 min at 78 km/h, then 1 min at 46 km/h, and finally rested for 0.5 min.

The Deep Keen Bend data set was collected while the subjects were performing the deep squat exercise. At the time of acquisition, subjects rested for 0.5 min at the beginning and end of the acquisition. At other times, subjects performed the squat exercise for 3 min. Before starting the squat, the subject straightens the back and lower back with the knees aligned with the tips of the toes. The squat was performed in a natural and fluid manner, with hands on the knees when the lowest point of the squat was reached, so that the hands could provide proper support when rising.

The Mixture dataset was collected from subjects performing a mixture of three movements, namely, handstands, arm swings, and squats. This data set contains four records. In each record, subjects rested for 0.5 min at the beginning and end of the acquisition. At other times, subjects performed two types of exercises for a total of 3 min. For the first type, subjects beckoned for 1.5 min and then swung their arms for 1.5 min. For the second type, the subject beckoned for 1.5 min and then squatted for 1.5 min. Of the four records, the first two were of the first type and the last two were of the second type.

4.2 Experimental Results and Analysis

In this paper, the performance of the algorithm was evaluated in five aspects: error, Bland Altman plot, Pearson coefficient scatter plot, heart rate estimation curve plot, and MA removal effect plot. Among the six methods compared in Table 1 (RandF, temko, TROIKA, JOSS, EEMD, and CorNet), there were some wild points, such as 70.18 for TROIKA. after removing outliers greater than 30 BPM, the mean errors of the five methods for all records were 3.25 BPM, 3.38 BPM, 3.52 BPM 7.66 BPM, 6.88 BPM, and 7.31 BPM. These results indicate that the performance of our method (DL + HMR + SR-based heart rate estimation) is still better (2.40 BPM) than these five methods even after removing the wild points in the six methods, which indicates that our method (DL + HMR + SR-based heart rate estimation) performs well and suggests that our algorithm (DL + HMR + SR) is effective in removing pseudo-periodic motion artifacts from the PPG signal.

To better compare different methods, Fig. 6 compares the F1 scores of different methods, that is, the average of the two types of F1 scores. For this method (emotion recognition based on BDA + ODA), the average F1 scores of all subjects are Dreamer's valence recognition is 0.69%, dreamer's arousal recognition is 0.65%, Amigos' valence recognition is 0.66%, and Amigos' arousal recognition is 0.63%. It can be seen from Fig. 6 that the F1 score of the method in this paper is higher than that of other methods (UDA is used to reduce the individual signal difference), which shows the advantages of the method in emotion recognition and shows that the algorithm in this paper (BDA + ODA) is better than other UDA algorithms in overcoming the individual signal difference of ECG [27]. Further, to better compare different methods, Figs. 7 and 8 show the confusion matrices for different methods to classify on Dreamer Valence and Dreamer Ambient, respectively. In the confusion matrix, each row represents the real class, and each column represents the prediction class. The elements (i, j) represent the percentage obtained when the samples originally belonging to class i are divided into class j. On the Dreamer dataset, the method in this paper (emotion recognition based on BDA + ODA)

Table 1 Error comparison between the method in this chapter and other heart rate estimation methods

Data set	User	Methods in this chapter	RandF	tcmko	TROIKA	JOSS	EEMD	CorNet
Running	S1	1.95	1.62	1.26	2.88	1.34	2.07	6.24
	S2	2.89	1.39	1.42	1.76	1.76	3.59	1.84
	S3	0.99	0.74	0.72	1.92	1.48	0.93	0.89
	S4	1.55	1.49	0.98	2.26	1.49	1.55	0.49
	S5	1.12	0.78	0.76	1.69	0.69	0.98	0.41
	S6	1.91	1.35	0.93	3.17	1.33	1.65	3.09
	S7	0.68	0.59	0.66	1.73	0.72	2.26	1.35
	S8	0.97	0.64	0.98	1.84	0.57	0.64	3.65
	S9	0.61	0.58	0.56	1.59	0.49	0.63	3.31
	S10	6.59	3.51	2.07	4.01	3.82	4.63	1.78
	S11	2.08	1.08	1.04	1.97	0.79	1.31	0.42
	S12	1.94	1.05	0.99	3.34	1.05	1.81	0.51
	Ave	1.93 ± 1.62	1.23 ± 0.81	1.02 ± 1.26	2.43 ± 0.79	1.28 ± 2.62	1.83 ± 1.22	1.99 ± 4.65
Beckoning	S1	2.14	2.88	2.21	4.08	17.45	2.05	5.81
	S2	1.72	3.81	4.81	2.66	22.61	1.68	7.25
	S3	1.98	3.52	2.82	2.82	4.88	2.41	14.54
	S4	1.58	2.29	3.43	3.94	32.11	23.03	6.84
	S5	2.02	3.23	1.63	70.19	4.76	3.64	7.35
	S6	2.67	2.36	2.36	3.82	25.59	2.83	4.99
	S7	2.74	3.68	2.59	20.73	8.22	4.27	5.99
	S8	2.31	5.87	3.13	2.89	3.59	2.31	7.01
	S9	1.59	2.37	1.85	2.49	5.32	1.89	4.94
	Ave	2.08 ± 0.94	3.33 ± 1.13	2.75 ± 0.97	10.62 ± 22.35	13.83 ± 10.81	4.89 ± 6.86	7.18 ± 2.91
Swing arm	S1	1.58	1.57	1.67	2.66	6.77	2.57	4.47
	S2	1.49	2.52	8.59	3.47	19.01	25.59	6.65
	S3	3.34	3.01	4.86	4.38	10.05	33.21	6.34
	S4	1.56	1.68	1.79	3.97	3.25	37.38	5.49
	S5	3.01	2.34	1.79	3.68	31.12	2.95	6.16
	S6	2.49	1.82	1.71	2.71	2.69	1.51	5.13
	S7	2.81	2.31	1.56	3.87	9.69	3.16	6.09
	S8	3.53	5.09	13.78	4.87	19.13	37.98	6.42
	S9	3.98	4.26	14.16	11.51	11.12	29.09	6.48
	Ave	2.64 ± 0.94	2.72 ± 1.22	5.54 ± 5.32	4.56 ± 2.71	12.53 ± 9.12	19.26 ± 16.32	5.93 ± 0.69
Elliptical trainer	S1	1.32	4.76	1.54	2.66	3.32	3.08	12.29
	S2	2.19	1.39	1.26	3.29	1.61	2.81	16.24
	S3	2.92	2.09	33.41	42.53	41.34	42.77	23.84
	S4	5.43	1.28	3.26	5.74	20.78	9.53	8.81
	S5	6.39	14.57	45.48	4.59	40.89	58.82	16.39
	S6	1.38	3.41	4.34	2.59	11.84	1.66	12.13
	S7	3.79	35.64	2.84	13.65	7.17	3.19	12.97
	S8	1.22	0.87	1.31	2.22	3.29	11.25	21.96
	S9	1.41	1.89	2.04	3.11	13.26	2.88	10.03
	Ave	2.89 ± 1.94	7.31 ± 11.45	10.60 ± 16.66	8.92 ± 13.09	15.93 ± 15.49	15.1 ± 20.89	15.07 ± 5.11

Table 1 (continued)

Data set	User	Methods in this chapter	RandF	tcmko	TROIKA	JOSS	EEMD	CorNet
Deep keen squat	S1	1.84	3.31	2.28	2.49	2.95	44.45	4.92
	S2	2.76	2.64	2.24	2.89	74.74	73.09	5016
	S3	3.43	36.57	1.92	3.89	11.76	53.32	4.77
	S4	2.76	14.29	34.98	3.91	7.45	25.82	3.89
	S5	1.38	1.97	1.56	3.13	15.44	2.67	3.19
	S6	3.89	5.24	31.51	3.91	4.59	51.99	9.19
	S7	3.15	8.75	21.03	2.59	4.73	59.28	10.19
	S8	3.75	14.27	16.74	5.67	70.92	27.04	12.94
	S9	1.09	1.47	3.28	1.98	4.04	4.36	12.05
	Ave	2.66 ± 1.03	9.83 ± 11.19	12.5 ± 13.04	3.38 ± 1.1	21.82 ± 29.14	37.99 ± 24.52	7.36 ± 3.74
Mixture	S1	4.13	3.53	4.29	5.05	9.58	16.27	7.32
	S2	2.01	1.91	1.85	2.39	2.89	2.23	6.19
	S3	1.37	3.76	1.76	2.23	2.79	1.55	9.73
	S4	1.93	2.09	2.36	2.56	1.98	8.03	13.04
	Ave	2.35 ± 1.22	2.81 ± 0.97	2.56 ± 1.18	3.05 ± 1.34	4.3 ± 3.54	17.4 ± 23.42	9.06 ± 3.04
Ave of all data (mean $\pm$ std)		2.4 ± 1.3	4.51 ± 7.13	2.55 ± 10.83	11.72 ± 15.98	11.72 ± 15.98	14.33 ± 19.37	7.31 ± 5.18
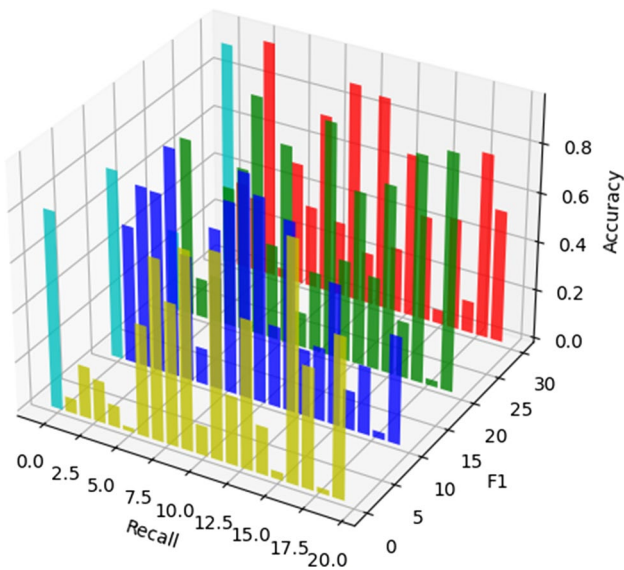
Fig. 6 F1 score of different emotion recognition methods

is 78.17% in positive emotion, 60.97% in negative emotion, and 57.12% in high arousal emotion, 79.32% in low arousal. Compared with other methods, this method performs better in valence classification and arousal classification, It shows that this method is superior to other methods (using UDA to reduce the individual signal difference) when it is used for emotion recognition, and it also shows that this algorithm (BDA + ODA) is superior to other UDA-based algorithms when it is used to eliminate the individual signal difference of ECG.

4.3 Heart Rate Estimation

On the data set Elliptic Trainer (Fig. 9), the estimated value deviates from the true value in 70–100 s. The reason may be that the trend of heart rate changes frequently, resulting in a large error in the heart rate peak tracking phase (when the heart rate value in the current time window is corrected based on the previous heart rate change trend). However, when the change trend of the rate of care is relatively stable, this method (heart rate estimation based on DL + HMR + SR) can accurately reestimate the heart rate. Moreover, in Fig. 9, the trend of heart rate estimation in the overall time is generally consistent with the trend of the real value, which indicates that the method in this paper performs a good heart rate estimation, thus demonstrating the effectiveness of the algorithm in this paper (DL + HMR + SR) in removing the pseudo-periodic motion artifacts in PPG.

5 Conclusion

Wearable devices monitor human health and emotions by collecting human physiological signals and based on physiological signal analysis and processing algorithms to effectively detect group music and dance well-being. First, we propose an algorithm based on sparse representation
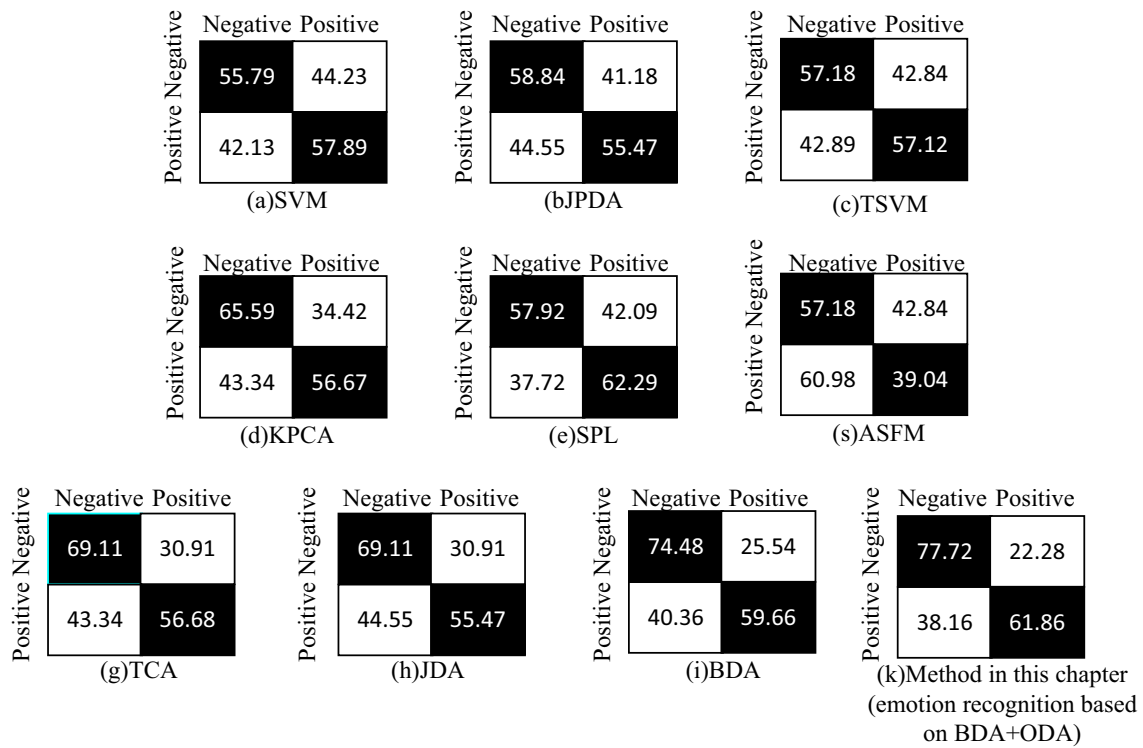
Fig. 7 Confusion matrix of different emotion recognition methods in Dreamer valence classification
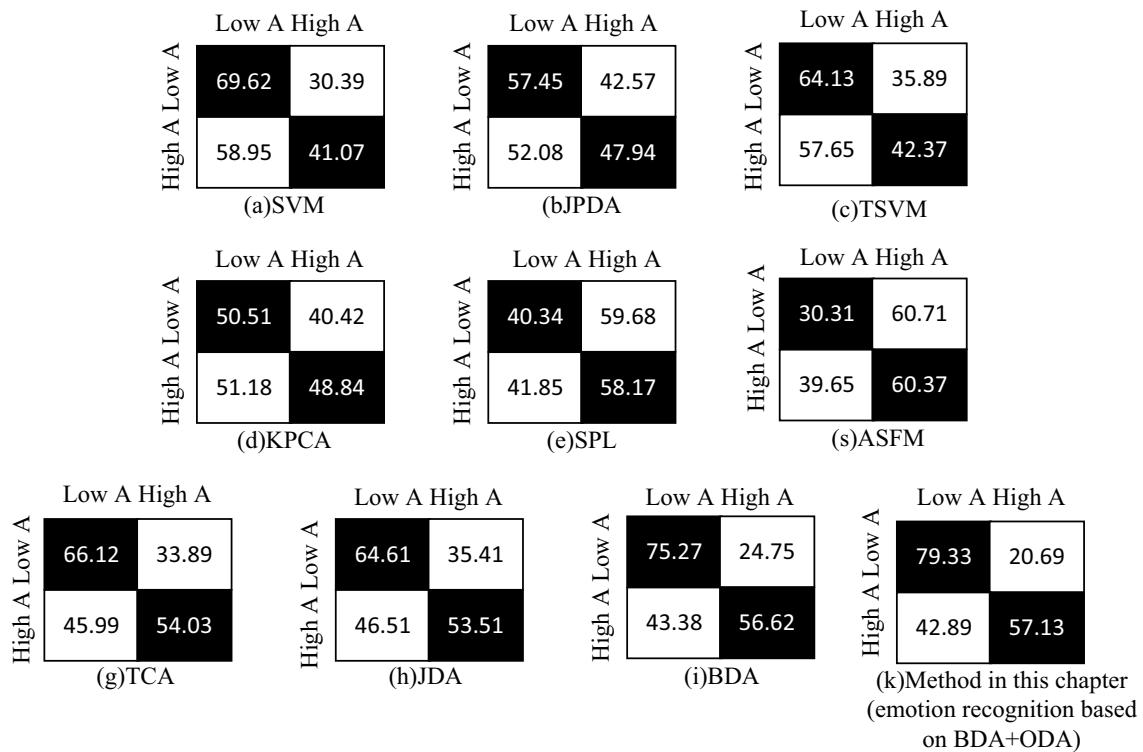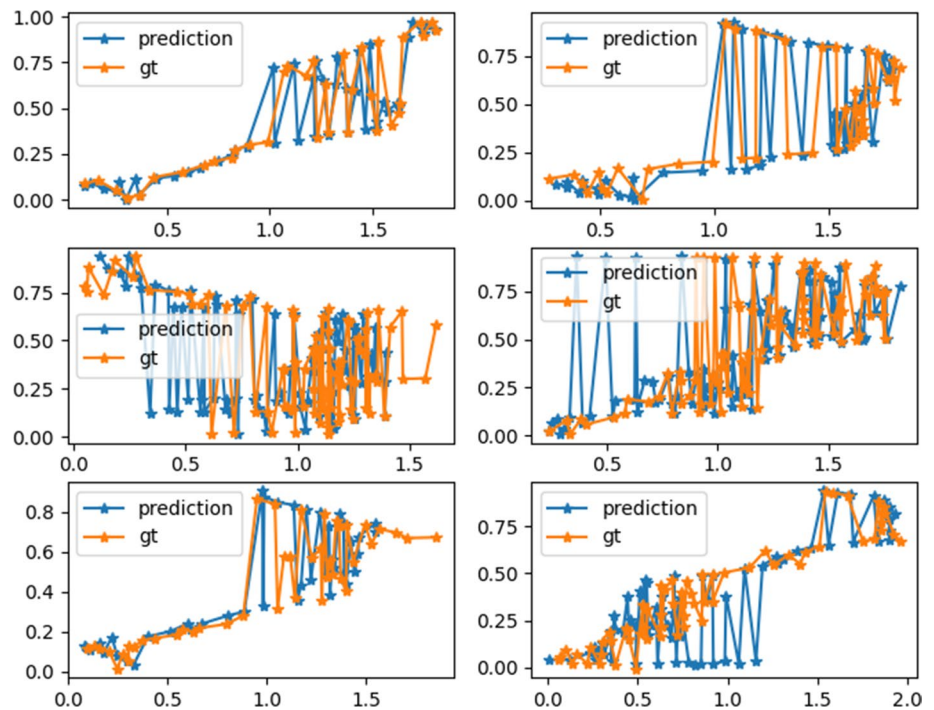
Fig. 8 Confusion matrix of different emotion recognition methods in Dreamer arousal classification

Fig. 9 The estimated heart rate curve of the method in this section (heart rate estimation based on DL+HMR+SR) on a subject record in six data sets

to eliminate motion artifacts of wearable PPGs. In addition, to address the problem of poor model generalization due to individual signal differences (between and within individuals) in human ECG signals, a wearable ECG individual signal difference elimination algorithm based on BDA is proposed. The effectiveness of the algorithm in eliminating ECG individual signal differences is verified in an emotion recognition experiment based on an open dataset. Our model can provide effective help for accurate estimation of emotions and group activities, not only limited to music and dance.

Data Availability The experimental data used to support the findings of this study are available from the corresponding author upon request.

Declarations

Conflict of Interest The authors declared that they have no conflicts of interest regarding this work.

Consent for Publication All authors reviewed the results, approved the final version of the manuscript, and agreed to publish it.

References

1. Lee, K., Lee, K.Y., Sheehan, L.: Hey Alexa! A magic spell of social glue?: Sharing a smart voice assistant speaker and its impact on users' perception of group harmony. Inf. Syst. Front. **22**(3), 563–583 (2020)
2. Lin, S., Zheng, B., Alexandropoulos, G.C., Wen, M., Chen, F., Mumtaz, S.: Adaptive transmission for reconfigurable intelligent surface-assisted OFDM wireless communications. IEEE J. Sel. Areas Commun. **38**(11), 2653–2665 (2020)
3. Lee, C.S., Wang, M.H., Tsai, Y.L., Ko, L.W., Tsai, B.Y., Hung, P.H., et al.: Intelligent agent for real-world applications on robotic edutainment and humanized co-learning. J. Ambient. Intell. Humaniz. Comput. **11**(8), 3121–3139 (2020)
4. Ji, B., et al.: A survey of computational intelligence for 6G: key technologies, applications and trends. IEEE Trans. Industr. Inf. **17**(10), 7145–7154 (2021)
5. Quasim, M.T., Alkhammash, E.H., Khan, M.A., Hadjouni, M.: Emotion-based music recommendation and classification using

machine learning with IoT Framework. Soft. Comput. **25**(18), 12249–12260 (2021)

6. Yan, Z., Zhou, J., Wu, Y., Liu, G., Luo, D., Zhou, Z., et al.: Shoes++ A smart detachable sole for social foot-to-foot interaction. Proc. ACM Interact. Mob. Wearable Ubiquitous Technol. **6**(2), 1–29 (2022)

7. Sun, Y., Xu, J., Wu, H., Lin, G., Mumtaz, S.: Deep learning based semi-supervised control for vertical security of maglev vehicle with guaranteed bounded airgap. IEEE Trans. Intell. Transp. Syst. **22**, 4431–4442 (2021)

8. Ben Sassi, I., Ben Yahia, S.: How does context influence music preferences: a user-based study of the effects of contextual information on users' preferred music. Multimedia Syst. **27**(2), 143–160 (2021)

9. He, G.: Schema interaction visual teaching based on smart classroom environment in art course. Int. J. Emerg. Technol. Learn. (iJET) **15**(17), 252–267 (2020)

10. Al-Turjman, F., Ever, E., Zahmatkesh, H.: Small cells in the forthcoming 5G/IoT: traffic modelling and deployment overview. IEEE Commun. Surv. Tutor. **21**(1), 28–65 (2018)

11. He, Y., Chernyshov, G., Han, J., Zheng, D., Thomsen, R., Hynds, D., et al.: Frisson waves: exploring automatic detection, triggering and sharing of aesthetic chills in music performances. Proc. ACM Interact. Mob. Wearable Ubiquitous Technol. **6**(3), 1–23 (2022)

12. Kaur, J., Sharma, A.: Establishing early foundations to promote emotional competence in preschool children. J. Appl. Soc. Sci. **16**(2), 399–418 (2022)

13. Shen, J., Xiao, L.D., Liu, Y., Zhang, H., Wu, L.: A phenomenological study on new care needs of maslow's need-hierarchy among disabled residents at nursing homes in modern Chinese society. J. Transcult. Nurs. **32**(5), 501–507 (2021)

14. Pareek, P., Thakkar, A.: A survey on video-based human action recognition: recent updates, datasets, challenges, and applications. Artif. Intell. Rev. **54**(3), 2259–2322 (2021)

15. Nie, L., Liu, M., Song, X.: Multimodal learning toward micro-video understanding. Synth. Lect. Image Video Multimedia Process. **9**(4), 1–186 (2019)

16. Hanur, B.S.: Children for future: gaining our children success through smart school of early childhood education. In: Proceedings of Annual Conference for Muslim Scholars, vol. 3, no. 1, pp. 644–653. (2019)

17. Lazarou, I., Stavropoulos, T.G., Meditskos, G., Andreadis, S., Kompatsiaris, I.Y., Tsolaki, M.: Long-term impact of intelligent monitoring technology on people with cognitive impairment: an observational study. J. Alzheimers Dis. **70**(3), 757–792 (2019)

18. Hong, X., Wu, Y.H.: The use of AR to preserve and popularize traditional Chinese musical instruments as part of the formation of the tourist attractiveness of the national art of Guizhou province. Digit. Scholarsh. Humanit. **37**(2), 426–440 (2022)

19. Özcan, E., Frankel, L., Stewart, J.: Uncommon music making: the functional roles of music in design for healthcare. Music Med. **11**(4), 245–255 (2019)

20. Mansir, F., Purnomo, H.: Islamic education learning strategies based on multiple intelligences in Islamic School. Psikis Jurnal Psikologi Islami **6**(1), 48–57 (2020)

21. Dozie, K.C.N., Uwaezuoke, U.M.: Properties of buys-ballot estimates for mixed model in time series decomposition. Galore Int. J. Appl. Sci. Humanit. **4**(2), 35–40 (2020)

22. Fukuie, T., Suwabe, K., Kawase, S., Shimizu, T., Ochi, G., Kuwamizu, R., et al.: Groove rhythm stimulates prefrontal cortex function in groove enjoyers. Sci. Rep. **12**(1), 1–14 (2022)

23. Riva, G., Mantovani, F., Wiederhold, B.K.: Positive technology and COVID-19. Cyberpsychol. Behav. Soc. Netw. **23**(9), 581–587 (2020)

24. Tabbaa, L., Searle, R., Bafti, S.M., Hossain, M.M., Intarasisrisawat, J., Glancy, M., Ang, C.S.: VREED: virtual reality emotion recognition dataset using eye tracking & physiological measures. Proc. ACM Interact. Mob. Wearable Ubiquitous Technol. **5**(4), 1–20 (2021)

25. Shiqi, Li.: The effect of square dance exercise on physical self-esteem and well-being of older adults, pp. 2–24. Zhengzhou University, Zhengzhou (2017)

26. Ye, W.: Patterns of the effects of group leisure sports on the well-being of older adults. J. Tianjin Inst. Phys. Educ. **32**(5), 455–460 (2014)

27. Sun, L., Liang, J., Zhang, C., Wu, D., Zhang, Y.: Meta-transfer metric learning for time series classification in 6G-supported intelligent transportation systems. IEEE Trans. Intell. Transport. Syst. (2023). https://doi.org/10.1109/TITS.2023.3250962

Publisher's Note Springer Nature remains neutral with regard to jurisdictional claims in published maps and institutional affiliations.